

EXPERIMENTAL EVALUATION OF THE INFLUENCE OF THE LEVEL OF THE GROUND WATER TABLE ON THE BEARING CAPACITY OF CIRCULAR FOOTINGS*

M. AJDARI** AND A. ESMAIL POUR

Dept. of Civil Eng., Fasa University, I. R. of Iran
Email: ajdari@fasau.ac.ir
Jondi Shahpoor Company, I. R. of Iran

Abstract– In this study, a bearing capacity device is designed and fabricated to determine the load-settlement behavior of three circular footing models resting above the ground water table. Capillary rise in the studied well graded sand is measured and the level of the water table is controlled at the desired heights during each bearing capacity test. Moreover, shear strength parameters and soil water retention curve of the soil are also determined.

Experimental results show that using the conventional equations available in the literature of foundation engineering to determine the bearing capacity of footings built above the ground water table can be highly conservative. Moreover, despite the conventional theories, lowering of the ground water table can result in a decrease in the bearing capacity of shallow foundations. Therefore, utilizing the in situ experiments such as cone penetration test performed while the ground water table is at its highest level can lead to a quite non-conservative estimation of the bearing capacity of footings. In addition, an empirical relationship is proposed to simulate the bearing capacity factor, N_γ , of circular footings based on the experimental results.

Keywords– Bearing capacity, circular footing, ground water table

1. INTRODUCTION

Determining bearing capacity of shallow footings has been one of the major interests of geotechnical engineering researchers for about a century [1]. In this regard, Terzaghi (1943) proposed Eq. (1) assuming the validity of the superposition principle [2]:

$$q_u = qN_q + cN_c + 0.5\gamma BN_\gamma \quad (1)$$

in which, q_u is the bearing capacity of footing, q is the surcharge pressure, c is the cohesion of the soil, γ is the unit weight of the soil, B is the footing width and N_γ , N_q and N_c are bearing capacity factors being functions of the internal friction angle. Terzaghi also reported that the soil water reduces the surcharge and the unit weight of the soil leading to a decrease in the bearing capacity of the footing [2]. Later researchers extended Eq. (1) to take the influence of the ground water on the bearing capacity of shallow footings into account [3-7]. Vesić recommended taking the highest ground water table (GWT) as the most conservative state in the analysis and design of footings [4]. In these studies, soil layers which lie above the GWT are assumed to be completely dry.

It is worth mentioning that the capillarity pressure exists in the fine-grained soils and also, the hydration potential of the particles of plastic clays, which are components of matric suction [8], draw water up from the GWT and a significant portion of the soil located beneath the footing usually possesses

*Received by the editors May 14, 2014; Accepted April 25, 2015.

**Corresponding author

a non-zero suction value. Matric suction may exist in either saturated or unsaturated parts of the soil and plays a major role in the shear strength of the material [9-11], considerably changing the bearing capacity of the soil. Broms reported an increase in the bearing capacity of flexible pavements built on a fine-grained soil with an increase in the suction value [12]. Further, Steensen-Bach et al.'s experimental results showed that the bearing capacity of an unsaturated sand is four to six times higher than that of the saturated sand [13].

There has been growing interest in the investigation of the bearing capacity of the unsaturated soil in the past two decades. Fredlund and Rahardjo and Oloo considered the role of matric suction in the shear strength of the soil as an additional cohesion and extended equation 1 to determine the bearing capacity of unsaturated soils [14, 15]. Jahanandish et al. used the zero extension line method to determine the bearing capacity of strip footings built on the unsaturated soils [16]. They assumed a uniform suction distribution within the plastic zone of the soil and provided several design charts to estimate the N_γ -parameter knowing the suction value and soil characteristics.

Besides, several experimental studies have been done in recent years to evaluate the load-deformation behavior of footings when soil suction is more than zero. Costa performed some plate load tests on the unsaturated Lateritic soil deposit and reported a non-linear decrease in the amount of plate settlement with an increase in the matric suction value [17]. Mohammed and Vanapalli performed several experimental tests using two square shaped footing models with the length of 100 and 150 mm resting on a coarse-grained soil [18]. The experimental results showed that the bearing capacity increases significantly with a suction increase and the conventional bearing capacity equations are highly conservative. Similar results were reported by Vanapalli et al. based on the experimental tests carried out using small square shaped footing models [19]. Schanz et al. performed similar experiments on a small surface strip footing model resting on Hostun sand and reported an initial increase in the bearing capacity with an increase in suction value followed by a decrease in the bearing capacity of the footing model surpassing the suction value corresponding to the inflection point of the soil water retention curve (SWRC) [20].

In this regard, the work of Fellenius and Altaee done on the scale effect on the stress-settlement response of soils is also worth mentioning [21]. Also, the studied matric suction in all these studies was limited to 15 kPa and the studied soils are classified as coarse-grained. Also, experimental results show that the capillary rise, elevation of the GWT and the dimension of the footing, all act to influence the bearing capacity of shallow footings. Therefore, further experimental investigations to perform a comprehensive evaluation of the various aspects of the load-settlement response of shallow footings built above the GWT are of great importance for safe and economical designs of structures in arid and semi-arid regions of the earth.

In this research, an extensive experimental program was carried out to determine how GWT affects the load-settlement and bearing capacity of circular footing models. The influence of the water level on the bearing capacity of surface footings is investigated over a wide range of matric suction (0 to 6000 kPa) and the results are discussed through a simple physical model of the mechanical behavior of unsaturated soils. Moreover, knowing the N_γ -parameter in saturated condition, harmonic average suction value of the soil in the influence depth of the footing, air entry suction of the soil, footing width and soil average unit weight, an alternative empirical equation proposed in this paper can estimate the bearing capacity factor, N_γ in the unsaturated condition. The fabricated equipment, experimental procedure, studied soil, and the tests results are described in the subsequent sections.

2. BEARING CAPACITY DEVICE

The special equipment needed to perform the load-settlement tests on circular footing models was designed and fabricated. Key elements of the equipment are indicated in Fig. 1 and the description of its details is as follows: The loading frame was constructed utilizing two UNP 50×150 steel profiles. The

end face of these profiles was completely welded to the base of the equipment to provide a rigid support which can resist against the subjected loads and to ensure the stability of the equipment during the loading process. In addition, a continuous beam supported by two hinges was used to mechanically load the footing models. A 4m long IPE 160 steel profile was used as the abovementioned beam. Distances between weights, footing models and the hinge support of the beam were selected such that the load applied on the model is 10 times more than the weights hung at the end of the beam. Moreover, a cylindrical solid steel profile with the diameter of 50 mm played the role of the load ram which transferred the imposed force to the load cell. A cylindrical hollow profile was also utilized as a horizontal support of the load ram that ensures the normality of the applied load to the footings. A load cell with the maximum load capacity of 50 kN was employed to measure the amount of the load applied on the footings, even after the collapse of the soil placed beneath the footing and the occurrence of a probable softening incident. The metal ring of the load cell was calibrated using the desired imposed loads. Two displacement gauges were directly placed on the surface of the footings to measure the average settlement of the model during the loading procedure. Also, two additional strip steel pieces were horizontally welded on the upper surface of the 90mm footing model to provide a suitable place for the displacement gauges.



- | | |
|---------------------------------------|---------------------------|
| 1- Loading Arm | 6- Displacement Gauge |
| 2- Loading Ram | 7- Circular Footing Model |
| 3- Loading Frame | 8- Test Tank |
| 4- Horizontal Support of the Load Ram | 9- Piezometer |
| 5- Load Cell | 10- Drainage Valve |

Fig. 1. Bearing capacity test device

The cylindrical test tank with a diameter of 900 mm and depth of 600 mm was made of the steel plate with a thickness of 6 mm. The diameter of the tank was selected large such that the boundary effect on the stress bulb generated by the footing is avoided. The required provisions for regulation of the GWT and eye

inspection of the soil including the water inlet, water outlet, drainage valves, a piezometer (12.5mm in diameter) and a transparent Plexiglas window were added to the tank. Several perforated cups were placed at various depths of the soil to validate the achievement of the desired relative density, and also, to determine the water content (and suction) profile in the soil mass.

Three steel circular plates with diameters of 90, 120 and 140mm and thickness of 12mm were used as the footing models. A small hole was engraved in the center of the plates to facilitate the placement of the load cell on the footing model and to provide a simple support, preventing any probable moment load being transferred to the footing model. Also, the engraved hole prevented any possible sliding of the load cell tip.

3. STUDIED SOIL

A well graded sand was employed to study the shear strength, SWRC and bearing capacity determination. Several classification tests were done using the ASTM (2000, 2002 and 2003) code procedure [22-25]. The index properties investigated in this study included the determination of specific gravity, optimum water content, maximum dry density, maximum and minimum relative densities. Table 1 shows the physical properties of the material. The maximum particle size used for preparing the sample was 10mm (obtained by sieving) which is small by comparison to the footing models size. The studied soil contains around two percent fine grains. Figure 2 demonstrates the particle size distribution curve of the soil. Size distribution parameters of the soil particles are also indicated in Table 1.

Table 1. Index properties of the studied soil

Parameter	Amount
Specific gravity (G_s)	2.65
Uniformity coefficient (C_u)	6.5
Coefficient of curvature (C_c)	1.8
USCS classification	SW
Optimum water content (%)	9.4
Maximum dry density from standard proctor test (kN/m^3)	20.06
Maximum void ratio (e_{max})	0.89
Minimum void ratio (e_{min})	0.32

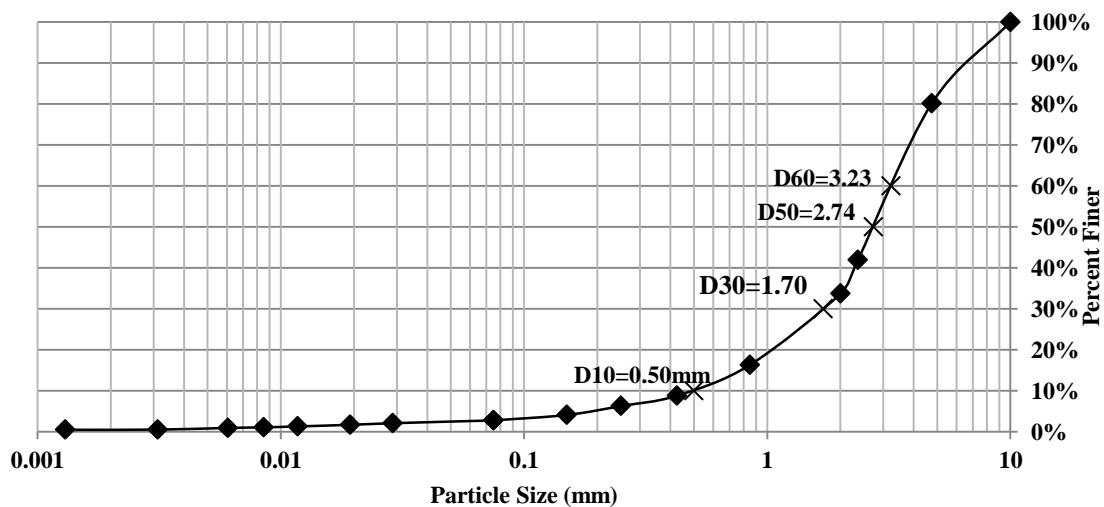


Fig. 2. Particle size distribution curve of the studied soil

Vesić reported that the general shear failure takes place at relative densities of more than 70% whenever the depth of footing is zero (i.e. surface footing) [4]. Variation of the relative density of the soil with the compaction effort was determined and the desired value was achieved before the loading process to ensure that the soil fails under the general shear failure mode. Maximum, minimum and desired void ratios are also indicated in Table 1.

Desorption branch of the SWRC was determined using the filter paper technique. This method is based on the principle that, when a wet soil is located close to a drier filter paper inside an air tight container the paper absorbs water from the soil until both soil and paper reach equilibrium of the suction value [26]. This water swap can take place by the vapor flow while soil and filter paper are not in contact, leading to a total suction (relative humidity) equalization between the soil sample and the filter paper. Moisture contents of the soil and the filter paper are determined after the suction equalization. Next, corresponding suction value is determined utilizing the adsorption branch of the water retention curve (WRC) of the paper. Although this method is simple and cheap, careful attention must be paid to the time allowed for reaching equilibrium of suction, and also temperature fluctuation to achieve reliable data measurements. It is notable that the SWRC depends on the stress state and initial soil structure, and therefore, sample preparation technique (e.g. compaction method, initial dry density and initial moisture content) may significantly change the curve. In this study, wet soil specimens taken from various depths of the test tank were placed in small sealed containers near Whatman filter paper n°42 for two weeks and the coincident suction values were calculated using the paper calibration curve presented by Fredlund and Rahardjo (1993) [14]. SWRC of the studied soil is indicated in Fig. 3. From this figure, air entry and residual suctions of the soil are approximately 15kPa and 6000kPa, respectively. This curve was also used to indirectly determine the suction profile within the soil mass during the load-settlement tests: water content profile was calculated utilizing the perforated cups placed at different depths of the soil and then, the corresponding suction profile was determined using the SWRC.

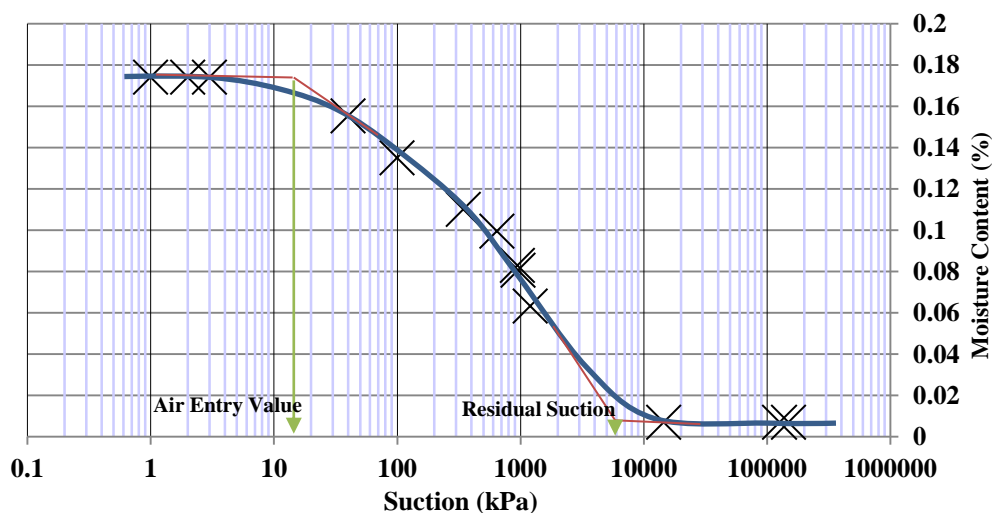


Fig. 3. Soil water retention curve determined from filter paper tests

Direct shear test deals with the determination of the consolidated drained shear strength of the material at different stress states [27]. The test is done by shearing the samples in a controlled strain rate device which is capable of imposing a shear force on the specimen along a predetermined shear plane parallel to the faces of the specimen [28]. The square shear box is divided vertically by a horizontal plane into two halves of equal thickness which are fitted together with two alignment bolts. The shear box is

also fitted with gap bolts which control the space between the top and bottom halves of the shear box and remove the frictional resistance that originates from the sliding of two halves of the box on each other. The normal force is applied by a loading yoke which is activated by desired weights and a calibrated load cell is used to determine the imposed shear force during the deformation of the specimen. Four saturated shear tests at vertical stresses of 50, 75, 100 and 150kPa were carried out in this study. The shearing rate presented by ASTM (D3080, 2003) was used [27]. The shear strengths of the samples versus applied normal stresses are shown in Fig. 4. Internal friction angle and the cohesion of the soil determined from this figure are 50.5° and 2kPa, respectively.

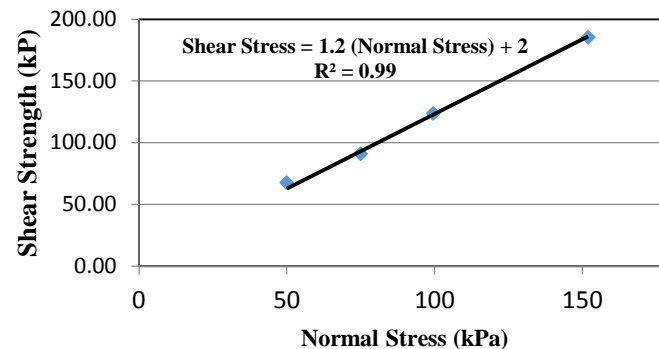


Fig. 4. Saturated shear strength of the soil versus normal applied stress

4. PROCEDURE OF THE LOAD-SETTLEMENT TESTS

The soil was uniformly placed in the tank in nine 60mm lifts through a funnel from a height of 25mm. The desired relative density of the soil was achieved by dynamic compaction of the soil utilizing a hand compactor (a 11kg weight) that fell freely from a height of 100mm on the soil. Also, a small 2.5kg weigh was used to compact the soil mass located beside the perimeter of the tank. Soil layers were compacted at the optimum water content (9.4%) and the dynamic compaction continued until the relative density of 85% was achieved. It is worth noting that the temperature was maintained at 25°C and the relative humidity of approximately 50% was recorded during compaction of the soil and the loading procedure.

As the first step of each test, the GWT was raised to the top of the soil employing the drainage valves and was kept in this condition for 24 hours to ensure the saturation of the soil mass. Next, the water table was lowered and raised using the outlet pipe and drainage valves three times to take the effect of the water table fluctuation into account. Finally, the GWT was adjusted at the desired level using the drainage valves of the equipment. Water level was then inspected by piezometer. The elevation of the GWT and the amount of capillary rise are also checked through eye inspection of the soil from the transparent window of the tank. An aquarium made of Plexiglas was also employed beside the bearing capacity tests to measure the amount of the capillary rise once more.

To determine the bearing capacity of footing models, they were axially loaded by weights hung at the end of the loading arm (the simply supported continuous beam). After each loading increment, the settlement rate of the footing was monitored until it approached zero (or became less than 0.01mm/min for at least thirty minutes) and the average settlement corresponding to the applied load was then recorded. This procedure was repeated until the soil collapse occurred. As previously mentioned, moisture content profile within the influence depth of the footing models (i.e. 1.5 times of the footing diameter) was determined using the perforated cups which had been placed at various depths of the soil before the compaction process was carried out and suction profile was then calculated from SWRC at the end of each bearing capacity test.

Three series of bearing capacity tests were performed in this study. First, saturated bearing capacity tests were carried out: The GWT was gradually raised up to the top of the soil to facilitate the air escaping from the pores and was kept at the soil surface for 24 hours before the loading process to ensure the saturation of the soil mass. Second, unsaturated bearing capacity tests were performed at a uniform suction distribution condition: Soil mass was compacted at the constant moisture content of 0.06 and then subjected to the incremental vertical applied loads to collapse. These two types of load settlement tests are known as the “uniform suction profile bearing capacity tests” in the next sections. Third, bearing capacity tests were done while the GWT was controlled at various levels: The water table was kept at the level of $H/D=0.5, 1.0$, etc. (Fig. 9) for 24 hours to achieve the suction equilibrium condition and suction profile within the footing influence depth was calculated at the end of the loading process. The details of the layout of the controlled GWT tests are indicated in Table 2.

Table 2. Layout of the controlled GWT bearing capacity tests

Footing diameter (mm)	GWT fluctuation before loading process	Level of GWT (H/D) during loading process					Determination of the suction profile after loading process
		0.5	1.0	1.5	2.0	2.5	
90	×	×	×	×	×	×	×
120	×	×	×	×	×	-	×
140	×	×	×	×	×	-	×

5. RESULTS AND DISCUSSION

a) Uniform suction profile bearing capacity tests

Load-settlement response of footing models resting on the saturated soil (zero suction condition) is shown in Fig. 5. It is clear that an increase in the dimension of the footing leads to deepening of the stress bulb, an enlargement in the plastic zone and an increase in the bearing capacity of the surface footing models as experimental results indicate. The variation of the bearing capacity with the footing dimension is indicated in Fig. 6. Peak strength value of the footing models presented in Fig. 5 was employed to produce this figure, indicating a non-linear relationship between the footing diameter and the bearing capacity value and contradicting the assumption included in the early studies [2-4]. This discrepancy is perhaps due to the variation of soil properties (e.g. unit weight) with depth.

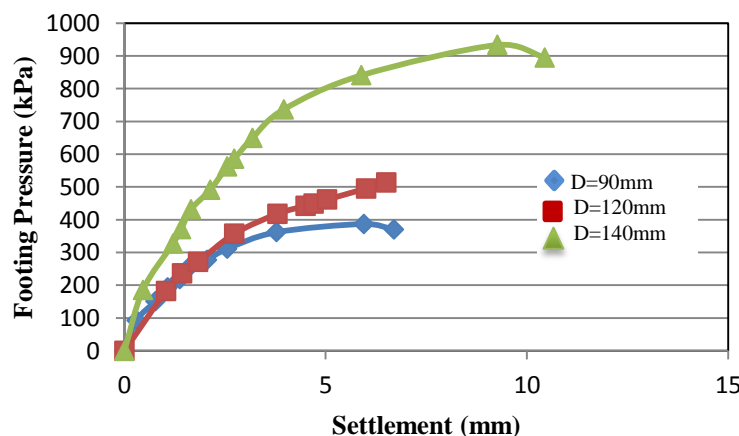


Fig. 5. Saturated load-settlement response of the circular footing models

Also, experimental results show that the collapse phenomenon took place in the relative settlements between 0.57 and 0.67, which corresponds to the general shear failure mode. Moreover, eye inspection of

the soil validates the extension of the sheared zone to the soil surface and occurrence of the general shear failure. Besides, pressure-settlement behavior of the footings exhibits a collapse incident followed by a softening behavior which verifies that the soil fails under the general shear failure mode (Fig. 5). Therefore, bearing capacity factor, N_γ , for studied surface footings ($q=0$) resting on the cohesion less saturated soil ($c \cong 0$) is simply calculated as follows:

$$N_\gamma = \frac{q_u}{0.5\gamma'Ds_\gamma d_\gamma} \tag{2}$$

where, D is the footing diameter, s_γ is the shape factor, d_γ is the depth factor and γ' is the buoyant unit weight of soil.

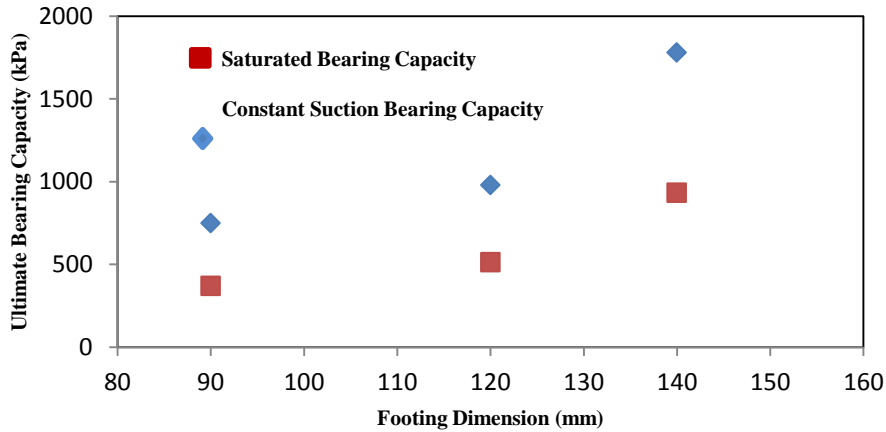


Fig. 6. Variation of the ultimate bearing capacity of the footing models with the footing dimension

As previously mentioned in the “Procedure of the Load-Settlement Tests” section, unsaturated bearing capacity tests were also performed at constant moisture content of 0.06. A six percent deviation from this moisture value was observed in the bearing capacity test performed on the 14cm footing model which is attributed to the experimental errors. Experimental results of the pressure-settlement response of footing models in the constant suction condition are shown in Fig. 7. All signs of the general shear failure were observed in the tests. The non-linear variation of the ultimate bearing capacity of unsaturated soils with footing dimension determined from Fig. 7 is re-plotted in Fig. 6 to compare with those of saturated soil. Obviously, for the studied suction value, bearing capacity of the unsaturated soil is about 2 times more than that of the saturated one. Although the mechanical behavior of the unsaturated foundations of buildings are influenced by the fluctuation of the GWT and depends on the various parameters such as footing diameter, capillary rise and level of the GWT, such experimental results provided from constant suction tests are useful in the economical design and analysis of footings built on the engineered embankments compacted at a constant water content condition in arid or semiarid areas.

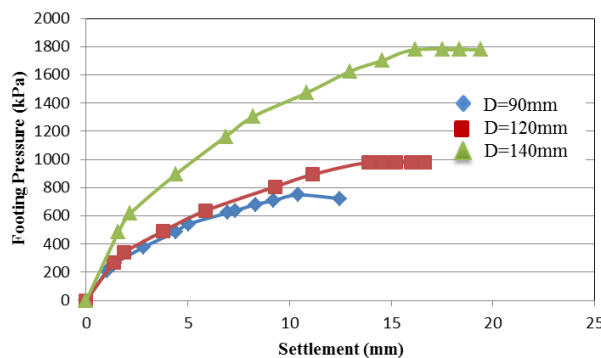
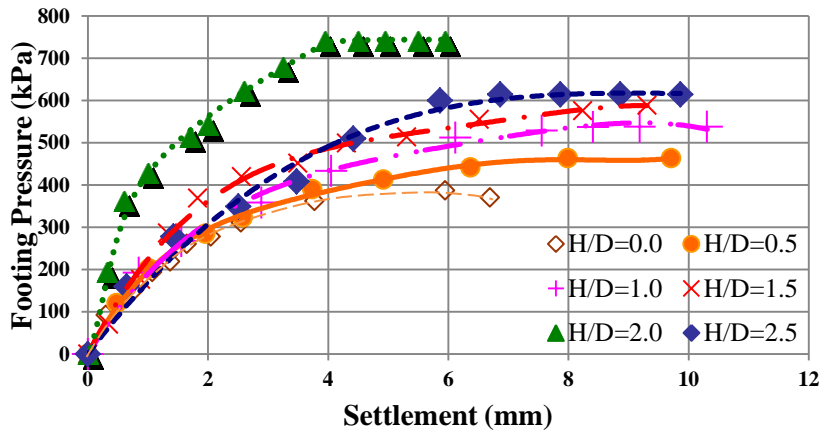


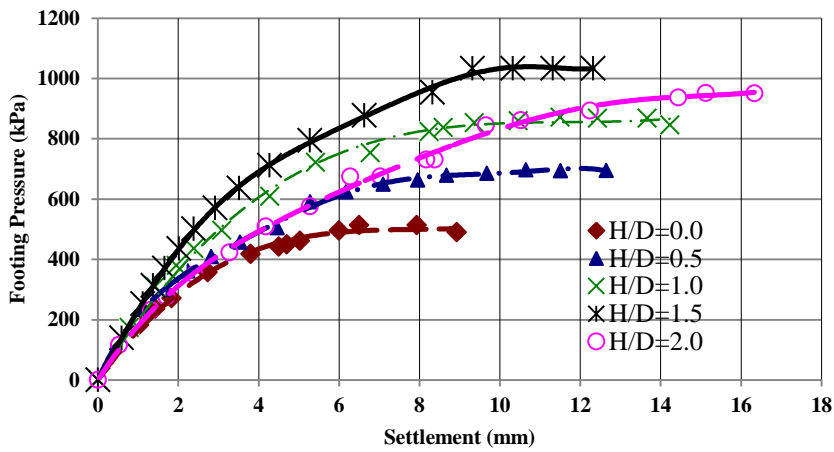
Fig. 7. Constant suction load-settlement response of the circular footing models

b) Controlled GWT bearing capacity tests

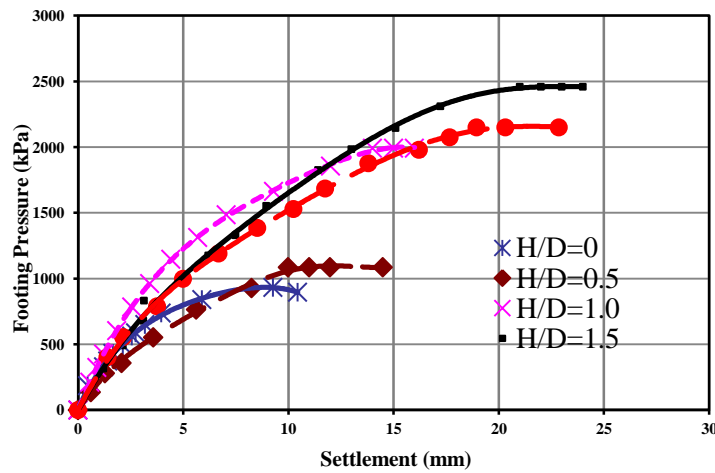
GWT was adjusted at various desired levels (Table 2) and then, load-settlement response of the footing models was evaluated. The results are indicated in Fig. 8. These outcomes indicate that a combination of three major parameters act to influence the bearing capacity of footings built above the GWT (Fig. 9):



(a)



(b)



(c)

Fig. 8. Controlled GWT bearing capacity tests results: (a) 90mm circular footing model (b) 120mm circular footing model (c) 140mm circular footing model

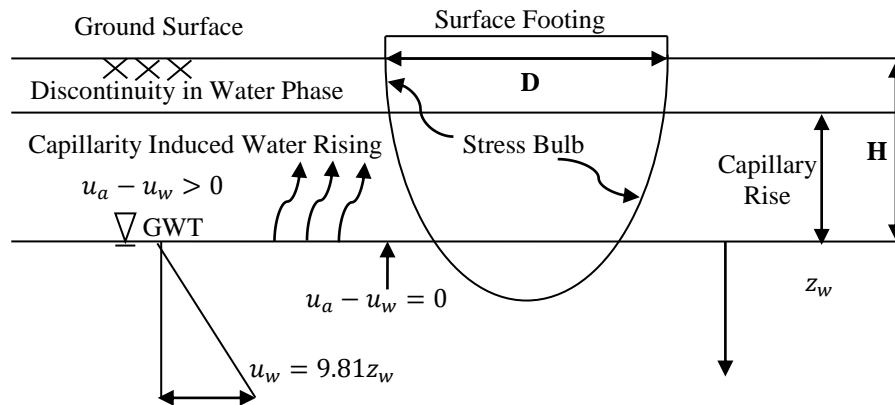


Fig. 9. Schematic presentation of the contribution of the capillary rise, GWT level and stress bulb in the bearing capacity of surface footings

i) The extension of the capillarity zone in which the pressure of the air-water interface ($u_a - u_w$) increases the effective stress (apparent cohesion) and shear strength of the soil [29], significantly affects the bearing capacity of the soil. The dimension of this zone depends on the soil type (SWRC parameters) and stress state. The height of this region is around 19cm for the studied soil. There is not a continuous water phase above the capillarity zone and hence, the effect of the matric suction is negligible in this region. Beneath the GWT, the amount of the matric suction is zero and the water pressure linearly increases with depth (Fig. 9).

ii) The influence depth of the footing and the expansion of the stress bulb are established by footing dimensions. The footing stress concentrates in the soil located near the footing surface and decreases with an increase in the depth. Therefore, the stress state of the soil placed close to the footing is more important in generating the bearing capacity of the footing.

iii) Fractions of the dry, unsaturated and saturated regions within the footing influence depth are specified by the level of GWT, capillary rise and footing dimension. These proportions state the average matric suction and shear strength of the soil.

The abovementioned argument explains the load-settlement behavior of the footing models presented in Fig. 8: The early increase in the bearing capacity with an increase in the depth of the GWT is due to the increase of the capillarity area placed in the influenced depth of the footing. The following decrease in the bearing capacity with an increase in the GWT depth is attributed to the replacement of the capillarity zone by the dry region and a decrease of the effective stress in the influence depth of the footing. This softening (the decrease in the bearing capacity of footings) commenced at the GWT depth around the capillary rise of the studied soil=19cm ($H/D=2$ for 9cm footing model and $H/D=1.5$ for 12cm and 14cm footing models, Fig. 9) which reconfirms the above mentioned explanation. Therefore, the uppermost level of the GWT is not necessarily the most conservative condition in the design of shallow footings and contradicting the assumption included in the theoretical relationships available in the literature [4], lowering the GWT can result in a decrease in the bearing capacity of shallow foundations. This discrepancy comes from the influence of the matric suction that exists in the capillarity zone which is not taken into account in the early studies.

Also, the early studies used the normalized GWT level (H/D , Fig. 9) to incorporate the effect of the ground water in the bearing capacity equation. The experimental results and some predicting equations available in the literature of foundation engineering are presented in Fig. 10. As previously mentioned, none of the equations can predict the decrease in the bearing capacity with an increase in the GWT depth. Further, test results show a non-linear relationship between the bearing capacity of footings and the normalized GWT depth, which contradicts some of the proposed equations. In addition, normalizing procedure indirectly included in these studies does not take all the various aspects of the load-settlement

behavior of the footings into consideration and different footing models have different curves in the normalized plane (Fig. 10). Besides, the matric suction included in the capillarity zone increases the shear strength of the soil and hence, the maximum bearing capacity values determined from the test outcomes is more than that predicted by the theoretical equations assuming a dry condition for the soil placed above the GWT.

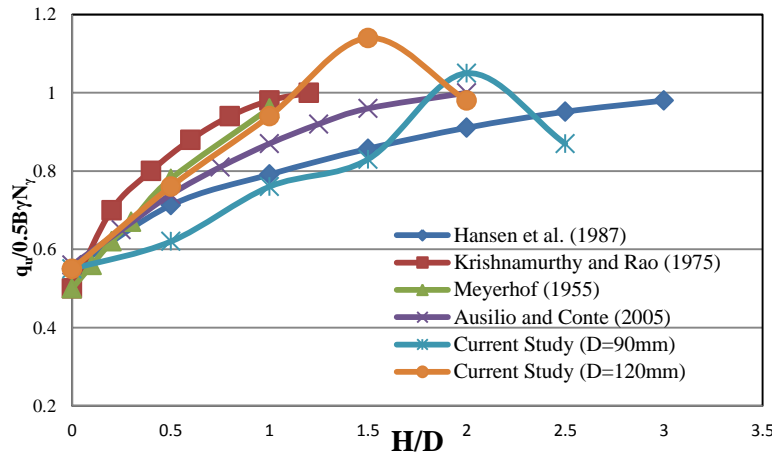


Fig. 10. Variation of the bearing capacity of footing models and normalized GWT level

c) Bearing capacity factor, N_γ

In this paper, a new empirical equation is proposed to predict the bearing capacity factor, N_γ , of footings built above the GWT utilizing the average suction value in the influence depth of the footing. To determine a realistic representative suction value of the soil, a harmonic average of the matric suction was calculated within the influence depth of the footing. Each measured suction value is assigned to an imaginary soil layer. The imaginary soil layers placed close to the footing are assigned larger weights in the averaging process and the deeper layers of the soil took lower weights, as presented in Eq. (3):

$$S_{ave,h} = \frac{ns_1 + (n-1)s_2 + \dots + 1 \times s_n}{n + (n-1) + \dots + 1} \quad (3)$$

where $S_{ave,h}$ is the harmonic average of the suction in the influence depth, n is the number of imaginary soil layers in the influence depth of the footing and s_i is the suction value in i^{th} imaginary soil layer numbering from the soil surface. The variation of the bearing capacity of the footing models with the harmonic average of the matric suction is shown in Fig. 11. The maximum bearing capacity corresponds to the suction value of approximately 1000kPa which is coincident to the inflection point of the SWRC. Similar result was reported by Schanz et al. (2010), although not mentioned by the authors [20]. This behavior can be explained as follows: first, increasing the suction value leads to an increase in the air-water interfacial area and an increase in the effective stress and shear strength of the soil. However, surpassing the medium range of matric suction, an increase in the suction value results in a decrease in the unsaturated pore water and eventually, a decrease in the air-water interfacial area which in turn, decreases the shear strength and bearing capacity of the soil. This figure also indicates that the fluctuation of the GWT has more influence on the bearing capacity of the larger footings such that the maximum bearing capacity ratio (unsaturated bearing capacity divided by saturated bearing capacity) for the larger and smaller footings equals 2.5 and 2, respectively (Fig. 11). This can be due to the inequality of the influence depth of the footings. In other words, larger footing ($B=14\text{cm}$) with a deeper stress bulb (i.e. influence depth= 21cm) incorporates the whole capillary rise (19cm) in the load-settlement process and the shallow

stress bulb (i.e. influence depth=13.5cm) of small footing (D=9cm) is extended only in a portion of the capillarity zone.

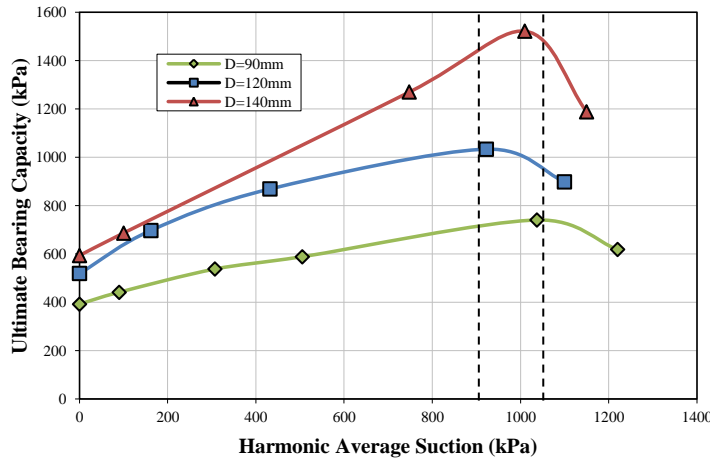


Fig. 11. Variation of the ultimate bearing capacity of the footing models with the harmonic average of the matric suction

The aforementioned results and explanations indicate the dependence of the bearing capacity factor, N_γ , on the combined effects of the footing dimension, average suction value (i.e. GWT level, capillary rise and footing dimension), SWRC parameters (i.e. capillary rise) and the soil unit weight (Eq. (2)), and therefore, the following empirical equation is proposed in this study to simulate N_γ -parameter:

$$\frac{N_\gamma^s}{N_\gamma^0} = \alpha \left(\frac{s_{ave,h}}{s_e} \right)^\beta \left(\frac{s_{ave,h}}{\gamma_{ave} D} \right) \tag{4}$$

in which N_γ^s and N_γ^0 are the bearing capacity factors at the harmonic average suction value of s and at the zero suction condition, respectively. s_e is the air entry suction of the soil determined from SWRC, γ_{ave} is the average unit weight of the soil in the footing influence depth, D is the footing diameter and α and β are fitting parameters. Bearing capacity factors were determined for the soil using the experimental outcomes and Eq. (2) and the proposed relationship (Eq. (4)) were then fitted to the experimental data points. α and β -parameters are 0.078 and -0.785 for the studied material. Experimental results and the proposed fitted curve are shown in Fig. 12. The accuracy of the proposed simulation is promising. More experimental investigations for developing two suitable relationships to predict the fitting parameters of Eq. (4) from basic characteristics of the soil are encouraged.

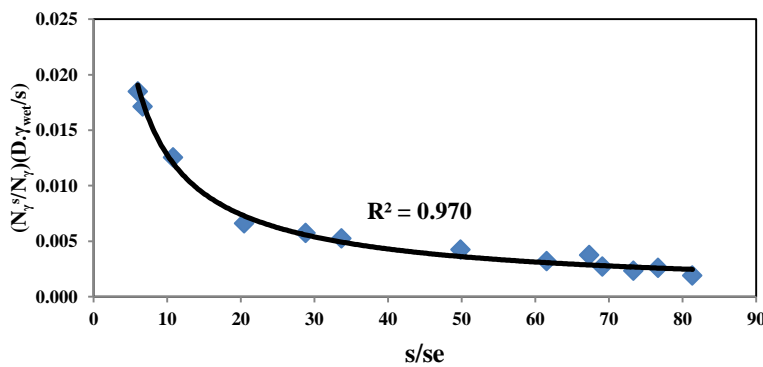


Fig. 12. Variation of the normalized unsaturated bearing capacity factor of the footing models with the normalized harmonic average of the matric suction

6. SUMMARY AND CONCLUSION

Thin layers of fine sand were compacted manually in a large test tank to reach a high relative density of 85%. Level of the ground water table was controlled by employing a water supply storage. A piezometer was utilized to precisely monitor the elevation of the water table and the transparent window of the tank wall facilitates the eye inspection of the capillary rise. Also, several rigid circular footing models were fabricated using the rolled steel plates. The diameter of footings was limited to 14 Cm. Footings were put on the surface of the soil and loaded incrementally using a loading ram. Bearing capacity and load-settlement behavior of the footings were determined. Moreover, SWRC of the soil was determined using the filter paper method and shear strength parameters of the soil were evaluated by saturated conventional direct shear tests.

Experimental results showed that the bearing capacity of footings resting above the GWT depends on several parameters such as capillary rise and average suction value in the footing influence depth, which are not included in the bearing capacity equations proposed in the literature. In addition, the highest GWT level is not necessarily the most conservative condition in the design and analysis of the footings and the earlier equations are not able to simulate the decrease in the bearing capacity of fine-grained soils by lowering the GWT. Also, an empirical equation to simulate the bearing capacity factor, N_γ , of shallow footings built above the GWT was proposed based on the experimental results. More researches for examining the role of the level of the GWT on the bearing capacity of fine grained soils are encouraged.

REFERENCES

1. Prandtl, L. (1921). On the penetrating strength (Hardness) of plastic construction materials and the strength of cutting edge. *Zeit. Agnew. Mathematical Mech*, Vol. 1, No. 1, pp. 15-20.
2. Terzaghi, K. 1943. *Theoretical soil mechanics*. Wiley, New York.
3. Meyerhof, G. G. (1955). Influence of roughness of base and ground-water conditions on the ultimate bearing capacity of foundations. *Geotechnique*, Vol. 5, pp. 227-242.
4. Vesic, A. S. (1973). Analysis of ultimate loads of shallow foundations. *Journal of the Soil Mechanics and Foundation Division, ASCE*, Vol. 99, pp. 45 -73.
5. Hansen, B., Denver, H. & Petersen, K. (1987). The influence of groundwater on bearing capacity of footings. *Proceedings of the 9th European Conference on SMFE*, Dublin, Vol. 2, pp. 685-690.
6. Bowles, J. E. (1996). *Foundation analysis and design*. Edition 5. McGraw - Hill, NY.
7. Ausilio, E. & Conte, E. (2005). Influence of groundwater on the bearing capacity of shallow foundations. *Canadian Geotechnical Journal*, Vol. 42, pp. 663- 672.
8. Ajdari, M., Habibagahi, G. & Masrouri, F. (2013). The role of suction and degree of saturation on the hydro-mechanical response of a dual porosity silt-bentonite mixture. *Applied Clay Science*, 83-84: 83-90.
9. Vanapalli, S. K., Fredlund, D. G., Pufahal, D. E. & Clifton, A. W. (1996). Model for the prediction of shear strength with respect to soil suction. *Canadian Geotechnical Journal*, Vol. 33, pp. 379-392.
10. Khalili, N. & Khabbaz, M. H. (1998). A unique relationship for χ for the determination of shear strength of unsaturated soils. *Geotechnique*, Vol. 48, No. 5, pp. 681-685.
11. Ajdari, M., Habibagahi, G. & Ghahramani, A. (2012). Predicting effective stress parameter of unsaturated soils using neural networks. *Computers and Geotechnics*, Vol. 40, pp. 89-96.
12. Broms, B. B. (1964). The effect of degree of saturation on the bearing capacity of flexible pavements. *Highway Research Record*, Vol. 71, pp. 1-14.
13. Steensen-Bach, J. O., Foged, N. & Steenfelt, J. S. (1987). Capillary induced stresses - fact or fiction? *9th ECSMFE, Groundwater Effects in Geotechnical Engineering*, Dublin, pp. 83-89.
14. Fredlund, D. G. & Rahardjo, H. (1993). *Soil mechanics for unsaturated soils*. 1st Ed. Wiley, New York.

15. Oloo, S. Y., Fredlund, D.G. & Gan, J. K. M. (1997). Bearing capacity of unpaved roads. *Canadian Geotechnical Journal*, Vol. 34, pp. 398-407.
16. Jahanandish, M., Habibagahi, G. & Veiskarami, M. (2010). Bearing capacity factor, N_γ , for unsaturated soils by ZEL method. *Acta Geotechnica*, Vol. 5, pp. 177-188.
17. Costa, Y. D., Cintra J. C. & Zornberg, J. G. (2003). Influence of matric suction on the of plate load tests performed on a lateritic soil deposit. *Geotechnical Testing Journal*, Vol. 26, No. 2, pp. 219-226.
18. Mohamed, F. M. O. & Vanapalli, S. K. (2006). Laboratory investigations for the measurements of the bearing capacity of an unsaturated coarse-grained soil. *Proceedings of 59th Canadian Geotechnical Conference*, Vancouver, BC.
19. Vanapalli, S. K., Sun, R. & Li, X. (2010). Bearing capacity of an unsaturated sand from model footing tests. *Proceedings of 5th Int Conf. on Unsaturated Soils*, Barcelona, pp. 1217-1222.
20. Schanz, T., Lins, Y. & Vanapalli, S. K. (2010). Bearing capacity of a strip footing on an unsaturated sand. *Proceeding of 5th Int Conf. on Unsaturated Soils*, Barcelona (Spain, 2011), pp. 1195-1200.
21. ASTM D4318-00, (2000). Standard test methods for liquid limit, plastic limit, and plasticity index of soils. Annual Book of ASTM Standards, 4(08), ASTM International, Philadelphia, PA.
22. ASTM D698-00a, (2000). *Standard test methods for laboratory compaction characteristics of soil using standard effort*. Annual Book of ASTM Standards, 4(08), ASTM International, Philadelphia, PA.
23. ASTM D854-02, (2002). *Standard test methods for specific gravity of soil solids by water pycnometer*. Annual Book of ASTM Standards, 4(08), ASTM International, Philadelphia, PA.
24. ASTM D422-63, (2003). *Standard test method for particle-size analysis of soils*. Annual Book of ASTM Standards, 4(08), ASTM International, Philadelphia, PA.
25. ASTM D5298, (1994). *Standard test method for measurement of soil potential (suction) using filter paper*. Annual Book of ASTM Standards, 4(08), ASTM International, Philadelphia, PA.
26. ASTM D3080, (2003). *Standard test method for direct shear test of soils under consolidated drained conditions*. Annual Book of ASTM Standards, 4(08), ASTM International, Philadelphia, PA.
27. Hamidi, A., Habibagahi, G. & Ajdari, M. (2013). A modified osmotic direct shear apparatus for testing unsaturated soils. *Getech. Test. J., ASTM*, Vol. 36, No. 1, pp. 1-10.
28. Fazeli, A., Habibagahi, G. & Ghahramani, A. (2009). Shear strength characteristics of Shiraz unsaturated silty clay. *Iranian Journal of Science & Technology, Transaction B: Engineering*, Vol. 33, No. 4, pp. 327-341.